

References 4–9 tabulate other examples. In polar systems bond energies are, in an absolute sense, not reliable, making careful orbital analyses necessary. For example, the calculated average carbonyl–metal binding energies in $\text{Ni}(\text{CO})_4$ and $\text{Fe}(\text{CO})_5$ are 51 and 78 kcal/mol, compared to 35 and 28 kcal/mol estimated from experimental considerations.²³

Registry No. $\text{Ni}(\text{CO})_4$, 13463-39-3; $\text{Fe}(\text{CO})_5$, 13463-40-6; $\text{Fe}_2(\text{CO})_6\text{C}_2\text{H}_2$, 60209-61-2; $\text{Co}_2(\text{CO})_6\text{C}_2\text{H}_2$, 12264-05-0.

References and Notes

- R. Mason and D. M. D. Mingos, *MTP Int. Rev. Sci.: Inorg. Chem., Ser. Three*, in press.
- F. A. Cotton, J. D. Jamerson, and B. R. Stultz, *J. Am. Chem. Soc.*, **98**, 1774 (1976); *J. Organomet. Chem.*, **94**, C53 (1975).
- W. G. Sly, *J. Am. Chem. Soc.*, **81**, 18 (1959); D. A. Brown, *J. Chem. Phys.*, **33**, 1037 (1960).
- A. B. Anderson, *J. Chem. Phys.*, **62**, 1187 (1975).
- A. B. Anderson, *J. Chem. Phys.*, **63**, 4430 (1975).
- A. B. Anderson, *J. Chem. Phys.*, **64**, 4046 (1976).
- A. B. Anderson, *J. Chem. Phys.*, **64**, 2266 (1976).
- A. B. Anderson, to be submitted for publication; T. N. Rhodin, C. B. Brucker, and A. B. Anderson, to be submitted for publication.
- A. B. Anderson, *J. Chem. Phys.*, in press.
- M. Elian and R. Hoffmann, *Inorg. Chem.*, **14**, 365 (1975).
- J. W. Cable and R. K. Sheline, *Chem. Rev.*, **56**, 1 (1956).
- G. Blyholder, *J. Phys. Chem.*, **68**, 2772 (1964).
- E. P. Kundig, D. McIntosh, M. Muskovitz, and G. A. Ozin, *J. Am. Chem. Soc.*, **95**, 7234 (1973).
- A. B. Anderson, *J. Mol. Spectrosc.*, **44**, 411 (1972).
- I. H. Hillier, M. F. Guest, B. R. Higginson, and D. R. Lloyd, *Mol. Phys.*, **27**, 215 (1974).
- L. Ley, S. P. Kowalczyk, F. R. McFeely, R. A. Pollak, and D. A. Shirley, *Phys. Rev. B*, **8**, 2392 (1973).
- B. Beagley, D. W. J. Cruickshank, P. M. Pinder, A. G. Robiette, and G. M. Sheldrick, *Acta Crystallogr., Sect. B*, **25**, 737 (1969).
- A. R. Rossi and R. Hoffmann, *Inorg. Chem.*, **14**, 1058 (1975).
- W. G. Fatley and E. R. Lippincott, *Spectrochim. Acta*, **10**, 8 (1957).
- Acetylene π^* + metal d orbital mixing causes the stretching: see F. R. Hartley, *Angew. Chem., Int. Ed. Engl.*, **11**, 596 (1972), and the following discussion.
- D. Thorn and R. Hoffmann, to be submitted for publication.
- A. B. Anderson and R. Hoffmann, *J. Chem. Phys.*, **60**, 4270 (1974).
- E. W. Abel, *Q. Rev., Chem. Soc.*, **17**, 139 (1963).

Contribution from the Department of Chemistry,
McGill University, Montreal, Quebec, Canada

Vibrational Spectra of the Pentacarbonyl(thiocarbonyl)metal(0) Complexes, $\text{M}(\text{CO})_5(\text{CS})$ ($\text{M} = \text{Cr}, \text{W}$) and $\text{trans-W}(\text{CO})_4(^{13}\text{CO})(\text{CS})$ (90% ^{13}C Enriched)¹

IAN S. BUTLER,*² AMELIA GARCIA-RODRIGUEZ, KEITH R. PLOWMAN, and C. FRANK SHAW III

Received April 27, 1976

AIC60307G

The vibrational spectra of the transition metal thiocarbonyl complexes, $\text{M}(\text{CO})_5(\text{CS})$ ($\text{M} = \text{Cr}, \text{W}$) and $\text{trans-W}(\text{CO})_4(^{13}\text{CO})(\text{CS})$ (90% ^{13}C enriched), have been studied and assignments are proposed for the fundamental modes on the basis of complete normal coordinate calculations. Many of the interaction constants used in these calculations were transferred directly from earlier work on the corresponding isoelectronic $\text{M}(\text{CO})_6$ species. For all three molecules, the average percent error between the observed and calculated frequencies is <1%, thus demonstrating the advantage of such force constant transfers between closely related species, as Jones et al. had predicted. Substitution of CS for CO in going from $\text{M}(\text{CO})_6$ to $\text{M}(\text{CO})_5(\text{CS})$ has no effect on the equatorial CO and M–C(O) force constants, $f_{\text{CO}^{\text{eq}}}$ and $f_{\text{MC}^{\text{eq}}}$; however, there are significant changes in the corresponding axial force constants, $f_{\text{CO}^{\text{ax}}}$ and $f_{\text{MC}^{\text{ax}}}$, the former increase while the latter decrease. In addition, the M–C(S) force constants, $f_{\text{MC}^{\text{s}}}$, are appreciably larger than any of the M–C(O) force constants. These results are in complete agreement with the stronger metal–carbon bonding found experimentally for metal–C(S) vs. metal–C(O) linkages. Also, the weakening of the M–C bonds trans to CS in the $\text{M}(\text{CO})_5(\text{CS})$ species is in accord with the chemistry of these molecules and is attributed primarily to the stronger π -acceptor capacity of the CS ligand.

Introduction

Numerous transition metal thiocarbonyls have been synthesized since the initial discovery of this class of complexes 10 years ago.^{3,4} Much of the recent interest in these complexes has focused on the comparative bonding properties of the CO and CS ligands.⁵ Since vibrational spectra reflect the internal forces and thus the bonding in molecules, we have undertaken a broad study of the complete vibrational spectra of transition metal thiocarbonyls in order to compare the spectra with those of structurally related metal carbonyls. To date, only two such studies have been reported: (a) $(\eta^6\text{-C}_6\text{H}_5\text{CO}_2\text{Me})\text{Cr}(\text{CO})_2(\text{CS})$ and $(\eta^6\text{-C}_6\text{H}_5\text{CO}_2\text{Me})\text{Cr}(\text{CO})_3$;⁶ (b) $\eta^5\text{-C}_5\text{H}_5\text{Mn}(\text{CO})_2(\text{CS})$, $\eta^5\text{-C}_5\text{H}_5\text{Mn}(\text{CO})(\text{CS})_2$, and $\eta^5\text{-C}_5\text{H}_5\text{Mn}(\text{CO})_3$.⁷ In both cases, detailed vibrational assignments were proposed.

The group 6B metal thiocarbonyl complexes, $\text{M}(\text{CO})_5(\text{CS})$, have been reported recently.^{8,9} Since extensive normal coordinate calculations have been carried out for the analogous $\text{M}(\text{CO})_6$ species,¹⁰ we felt that it would be particularly worthwhile investigating the vibrational spectra of the $\text{M}(\text{CO})_5(\text{CS})$ complexes in order to determine the transferability of force constants between these octahedral molecules. According to Jones et al.,¹⁰ many of the interaction constants for the $\text{M}(\text{CO})_6$ species should be directly transferable to other metal carbonyls, and this should be particularly true for the $\text{M}(\text{CO})_5(\text{CS})$ molecules because of the iso-

electronic nature of the CO and CS ligands. Furthermore, because of the larger mass of sulfur relative to oxygen, the CS vibrations will be more highly coupled with the metal–carbon modes than is the case for the CO vibrations. This means that energy factoring of the CS vibrational modes will be a poor approximation and such calculations will lead to force constants which are not reliable measures of CS bond strengths. More complete calculations are essential to obtain such information.

In this paper, we report the results of a vibrational analysis of the spectra of the $\text{Cr}(\text{CO})_5(\text{CS})$ and $\text{W}(\text{CO})_5(\text{CS})$ molecules and the mono- ^{13}C substituted derivative, $\text{trans-W}(\text{CO})_4(^{13}\text{CO})(\text{CS})$ (90% ^{13}C enriched). We have attempted to define the valence force constants for both metal thiocarbonyls in order to obtain a quantitative description of the bonding in them. These results are discussed in the light of the known chemistry of the complexes.

Experimental Section

The yellow, crystalline samples (~100 mg) of the metal thiocarbonyls were generous gifts from Professor R. J. Angelici and Mr. B. D. Dombek (Department of Chemistry, Iowa State University of Science and Technology, Ames, Iowa 50010) and were prepared by the literature methods indicated: $\text{M}(\text{CO})_5(\text{CS})$ ($\text{M} = \text{Cr}, \text{W}$)^{8,9} and $\text{trans-W}(\text{CO})_4(^{13}\text{CO})(\text{CS})$.¹¹

Infrared spectra were recorded on a Perkin-Elmer Model 521 grating spectrophotometer; the sampling conditions employed are given

Table I. Observed Fundamental Modes (cm^{-1}) for $\text{M}(\text{CO})_5(\text{CS})$ ($\text{M} = \text{Cr}, \text{W}$) and $\text{trans-W}(\text{CO})_4(^{13}\text{CO})(\text{CS})$

Symmetry type and vib no. ^a	$\text{Cr}(\text{CO})_5(\text{CS})$			$\text{W}(\text{CO})_5(\text{CS})$				$\text{trans-W}(\text{CO})_4(^{13}\text{CO})(\text{CS})$		
	Raman		Ir	Raman		Ir	Raman	Ir		Raman
	Ir Vapor ^b	Solid		CH_2Cl_2 soln	Vapor ^b			CH_2Cl_2 soln ^c	Solid	
a ₁ species (ir/Raman active)										
ν_1	2097 ms	2090 mw	2092 p	2102 m	2099 m	2096 vw	2097 p	2102 mw	2095 m	2091 w
ν_2	2032 s	2011 mw ^d	2024 p	2017 m	2007 ms	2003 w ^d	2015 p	1979 ms	1965 m	1954 w
ν_3	1280 s	1260 vw		1286 s	1272 s	1261 vw	1269 p	1284 ms	1265 s	1264 vw
ν_4	669 w	680 w		569 m ^e		573 vvw		571 mw	570 w	574 vvw
ν_5		424 m ^e	420 p	425 vw		426 s	423 p			425 s
ν_6	378 w	381 m	379 p			380 m	372 p			371 s
ν_7		351 s	346 p	339 w		346 m	337 p			345 m
ν_8		93 ms								
a ₂ species (inactive)										
ν_9	(364) ^f									
b ₁ species (Raman active)										
ν_{10}		2030 w				2025 vw				2022 vw
ν_{11}		512 vw				518 vvw				513 vvw
ν_{12}		390 m				412 vw				
b ₂ species (Raman active)										
ν_{14}		526 vvw ^e				479 vw				
e species (ir/Raman active)										
ν_{16}	2007 vs	2011 mw ^d		2002 s	1994 s	2003 w ^d		2006 s	1983 s	2008 mw
ν_{17}	649 s	659 w		569 m					563 w	564 vw
ν_{18}		526 vvw ^e				491 vw				483 w
ν_{19}		489 w		461 vw		463 w				463 w
ν_{20}	424 s	424 m ^e		368 m		375 m				
ν_{21}	341 w	339 w	339 dp			332 vw				331 vw

^a The δ (CMC) modes ($\nu_8, \nu_{13}, \nu_{15}, \nu_{22}, \nu_{23}, \nu_{24}$) are all expected to appear below 100 cm^{-1} . The far-ir spectra were not studied and since we experienced problems with scattering from the glass capillaries below 100 cm^{-1} , no Raman data are reported for these modes, except for ν_8 in $\text{Cr}(\text{CO})_5(\text{CS})$. ^b Using 10-cm gas cells fitted with CsI windows (KBr for the ^{13}CO derivative) and heated to $\sim 50^\circ\text{C}$. ^c Using a pair of matched 0.1-mm KBr solution cells. ^d Probable coincidence of ν_2 and ν_{16} in the Raman with the major contribution being from ν_2 , as symmetric modes are generally the most intense. ^e The calculations suggest that several pairs of modes will be accidentally degenerate, viz., $\text{Cr}(\text{CO})_5(\text{CS})$ (ν_5, ν_{20} and ν_{14}, ν_{18}) and $\text{W}(\text{CO})_5(\text{CS})$ (ν_4, ν_{14}). ^f Calculated from the first overtone observed at 728 w cm^{-1} .

in the footnotes to Table I. The spectra were calibrated against the $2139.4, 2119.7,$ and 2115.6 cm^{-1} bands of gaseous CO, the 1312.5 and 1226.2 cm^{-1} bands of indene, and the 679.2 and 633.9 cm^{-1} bands of atmospheric CO_2 . The accuracy of the measured frequencies is considered to be at least $\pm 1 \text{ cm}^{-1}$.

Raman spectra were obtained with a Jarrell-Ash Model 25-300 spectrometer using the 647.1 nm line of a Coherent Radiation Ltd. Kr^+ laser (Model 52K) for excitation. The power at the samples was usually $\sim 50 \text{ mW}$. The samples were sealed in Pyrex capillaries and were cooled to ca. -50°C by a cold nitrogen gas flow. Partial Raman spectra of CH_2Cl_2 solutions of the $\text{M}(\text{CO})_5(\text{CS})$ complexes were also recorded; complete spectra proved impossible to obtain owing to photochemical decomposition of the complexes upon prolonged exposure to the laser beam. All the spectra were calibrated against the emission lines of a neon lamp with an accuracy of about $\pm 1 \text{ cm}^{-1}$.

Normal coordinate calculations were carried out using two computer programs, WMAT and OVEREND, originally written by Overend et al.¹² but modified for use on the McGill University IBM 360/75 computer. In the least-squares refinement of the force constants performed by OVEREND, the observed frequencies are weighted as $1/\lambda_i = \text{const}/\nu_i^2$, and for the results reported here the additional weighting factor, $1/(\Delta\nu_i)^2$, was used where $\Delta\nu_i$ is the estimated error in the observed frequency, ν_i . As yet, the crystal structures of the $\text{M}(\text{CO})_5(\text{CS})$ complexes are unknown. However, preliminary x-ray diffraction data on $\text{Cr}(\text{CO})_5(\text{CS})$ have shown that this species is isomorphous with the $\text{M}(\text{CO})_6$ complexes [space group $Pna2_1$ (C_{2v}^9); $Z = 4$].¹³ Moreover, in the x-ray structures of metal thiocarbonyls which have been reported,^{14,15} the CS ligands are bonded to the metals via the carbon atoms and the metal-C-S linkages are essentially linear. Therefore, in order to obtain the C-S and M-C(S) distances necessary for the normal coordinate calculations on the $\text{M}(\text{CO})_5(\text{CS})$ molecules, the known bond lengths in $[\text{Ir}(\text{CO})_2(\text{CS})(\text{PPh}_3)_2]\text{PF}_6 \cdot \text{Me}_2\text{CO}$ ¹⁵ were used to calculate C-S/C-O and Ir-C(S)/Ir-C(O) ratios. These ratios were then employed as multiplicative factors to generate the appropriate C-S and M-C(S) distances using the same C-O and M-C(O) distances as Jones et al.¹⁰ did in their work on the $\text{M}(\text{CO})_6$ species. The distances actually used in the normal coordinate calculations were: (a) for $\text{Cr}(\text{CO})_5(\text{CS})$, Cr-C(O), 1.916 ; C-O, 1.171 ;

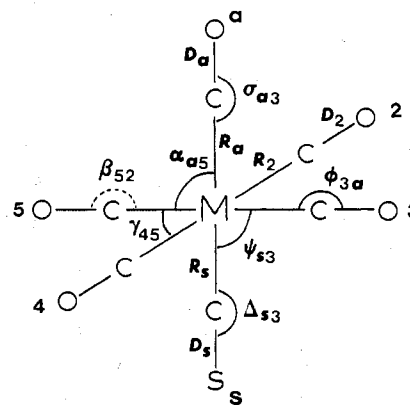


Figure 1. Internal coordinates for the $\text{M}(\text{CO})_5(\text{CS})$ molecules.

The associated symmetry coordinates are as follows. (a₁ block): $S_1 = 1/2(D_2 + D_3 + D_4 + D_5), S_2 = D_a, S_3 = D_s, S_4 = 1/2(\phi_{2a} + \phi_{3a} + \phi_{4a} + \phi_{5a}), S_5 = R_a, S_6 = 1/2(R_2 + R_3 + R_4 + R_5), S_7 = R_s, S_8 = 1/8^{1/2}(\alpha_{a2} + \alpha_{a3} + \alpha_{a4} + \alpha_{a5} - \psi_{s2} - \psi_{s3} - \psi_{s4} - \psi_{s5})$; (a₂ block): $S_9 = 1/2(\beta_{23} + \beta_{34} + \beta_{45} + \beta_{52})$; (b₁ block): $S_{10} = 1/2(D_2 - D_3 + D_4 - D_5), S_{11} = 1/2(\phi_{2a} - \phi_{3a} + \phi_{4a} - \phi_{5a}), S_{12} = 1/2(R_2 - R_3 + R_4 - R_5), S_{13} = 1/8^{1/2}(\alpha_{a2} - \alpha_{a3} + \alpha_{a4} - \alpha_{a5} - \psi_{s2} + \psi_{s3} - \psi_{s4} + \psi_{s5})$; (b₂ block): $S_{14} = 1/2(\beta_{23} - \beta_{34} + \beta_{45} - \beta_{52}), S_{15} = 1/2(\gamma_{23} - \gamma_{34} + \gamma_{45} - \gamma_{52})$; (e block): $S_{16a} = 1/2(D_2 + D_3 - D_4 - D_5), S_{17a} = 1/2(\beta_{23} + \beta_{34} - \beta_{45} - \beta_{52}), S_{18a} = 1/2^{1/2}(\sigma_{a2} + \sigma_{a3}), S_{19a} = 1/2^{1/2}(\Delta_{s2} + \Delta_{s3}), S_{20a} = 1/2(R_2 + R_3 - R_4 - R_5), S_{21a} = 1/2(\phi_{2a} + \phi_{3a} - \phi_{4a} - \phi_{5a}), S_{22a} = 1/2(\alpha_{a2} + \alpha_{a3} - \alpha_{a4} - \alpha_{a5}), S_{23a} = 1/2(\gamma_{23} - \gamma_{45}), S_{24a} = 1/2(\psi_{s2} + \psi_{s3} - \psi_{s4} - \psi_{s5})$.

Cr-C(S), 1.856 ; C-S, 1.498 \AA ; (b) for $\text{W}(\text{CO})_5(\text{CS})$, W-C(O), 2.059 ; C-O, 1.148 ; W-C(S), 1.985 ; C-S, 1.469 \AA .

The internal and symmetry coordinates for $\text{M}(\text{CO})_5(\text{CS})$ used in the calculations are defined in Figure 1. We have retained the nomenclature given in the $\text{M}(\text{CO})_6$ work¹⁰ but, because of the lower molecular symmetry of the metal thiocarbonyls, additional coordinate types had to be introduced. A detailed description of the force constant

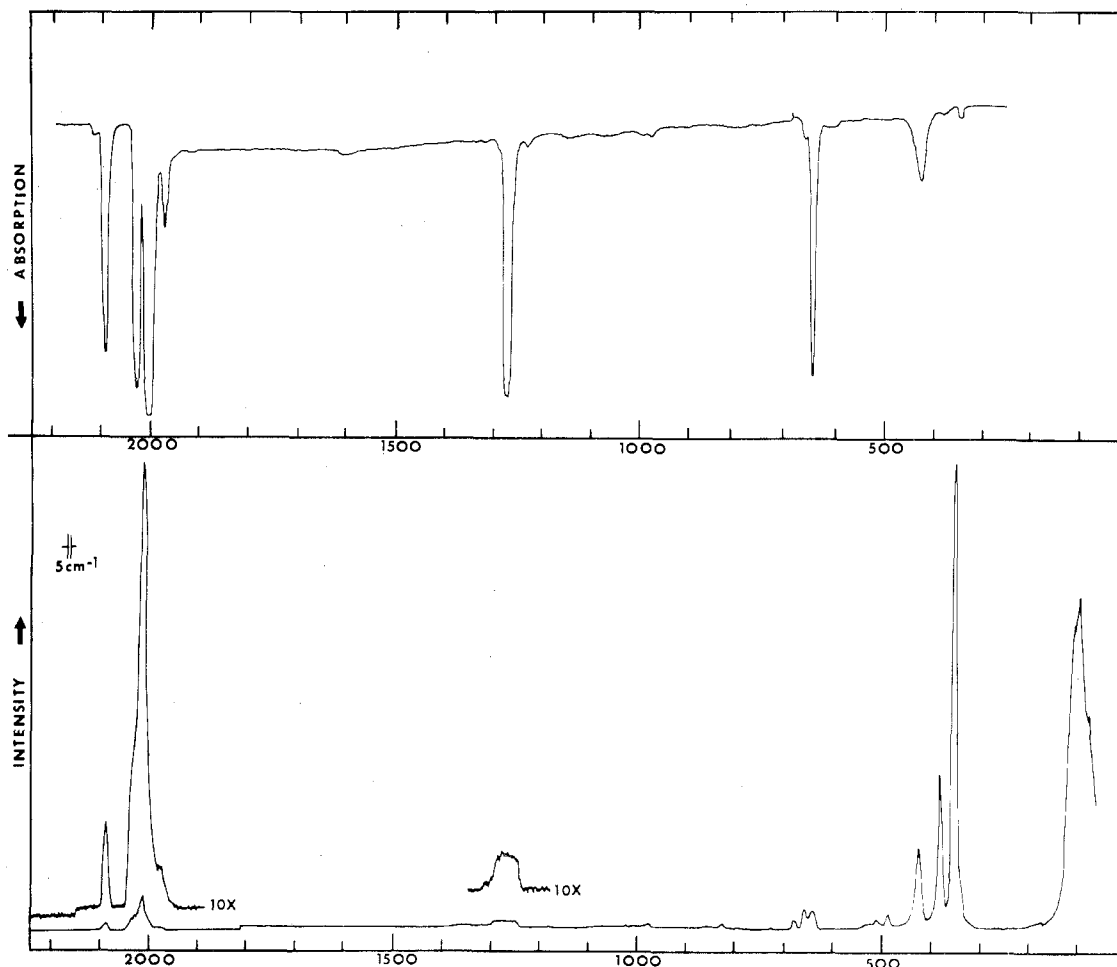


Figure 2. Vapor-phase ir and solid-state Raman spectra of $\text{Cr}(\text{CO})_5(\text{CS})$ in the fundamental regions. Experimental conditions: (ir) 10-cm gas cell with CsI windows, $\sim 50^\circ\text{C}$; (Raman) slit widths 5 cm^{-1} , Kr^+ excitation, 647.1 nm (50 mW), -50°C .

nomenclature is also given in ref 10, and we have retained this with only the following modifications: the superscripts ax , eq , and s denote the force constants associated respectively with the CO group trans to CS, the CO groups cis to CS, and the CS group itself.

Results and Discussion

The positions, relative intensities, and proposed assignments for the fundamentals of the $\text{M}(\text{CO})_5(\text{CS})$ and *trans*- $\text{W}(\text{CO})_4(^{13}\text{CO})(\text{CS})$ molecules are given in Table I. Some typical gas-phase ir and solid-state Raman spectra are shown in Figures 2 and 3.

From previous partial solution and gas phase ir studies,^{8,9,16} the $\text{M}(\text{CO})_5(\text{CS})$ molecules possess C_{4v} symmetry. The vibrational representation for an isolated $\text{M}(\text{CO})_5(\text{CS})$ molecule of this symmetry spans the modes indicated in eq 1, where the spectral activities of these modes are shown in parentheses.

$$\Gamma_{\text{vib}}^{C_{4v}} = 8 a_1 (\text{ir/Raman}) + a_2 (\text{inactive}) + 4 b_1 (\text{Raman}) + 2 b_2 (\text{Raman}) + 9 e (\text{ir/Raman}) \quad (1)$$

The correlation between these 24 modes and the 13 modes for the $\text{M}(\text{CO})_6$ species is shown in Figure 4. The frequency data for the metal hexacarbonyls were taken from the work of Jones et al.¹⁰ The $\text{M}(\text{CO})_5(\text{CS})$ frequencies were calculated using the general quadratic valence force fields determined for the $\text{M}(\text{CO})_6$ molecules by Jones et al.¹⁰ but modified to reflect the anharmonic frequencies of the $\nu(\text{CO})$ modes. Also, the redundancy conditions for the $\text{M}(\text{CO})_6$ species require that a number of force constants be defined only as linear combinations. Therefore, we refined certain of the force constants involved in these redundancies to give best fits for the hexacarbonyl data. (The choice of force constants, $f_{\alpha\alpha}$,

which are constrained or refined, is arbitrary but necessary when working in internal coordinate space.) The results of these calculations, as well as the approximations concerned, are given in Table V; the assumption of zero values for some of the interaction constants is not critical. In the following discussion of the proposed assignments for the $\text{M}(\text{CO})_5(\text{CS})$ complexes, "calculated frequencies" refer to those predicted for the $\text{M}(\text{CO})_5(\text{CS})$ species using the hexacarbonyl force fields.

CO Stretching Region ($2150\text{--}1900\text{ cm}^{-1}$). From the correlation diagram in Figure 4, three ir-active ($2 a_1 + e$) and four Raman-active ($2 a_1 + b_1 + e$) modes are expected for the $\text{M}(\text{CO})_5(\text{CS})$ molecules in the CO stretching region. The assignment of the ir bands in this region is quite straightforward both from their relative intensities and their "calculated" positions. In the case of the gas-phase ir spectra, the strongest bands at $\sim 2005\text{ cm}^{-1}$ are clearly attributable to the $e \nu(\text{CO})$ modes (ν_{16}), while the other two bands at ~ 2100 and $\sim 2020\text{ cm}^{-1}$ are assigned to the two $a_1 \nu(\text{CO})$ modes, ν_1 and ν_2 , respectively. The ordering of these $a_1^{eq}(\nu_1)$ and $a_1^{ax}(\nu_2)$ modes is consistent with that in numerous other $C_{4v} \text{M}(\text{CO})_5\text{L}$ species where L is a monodentate ligand.^{17,18} The gas-phase ir bands of *trans*- $\text{W}(\text{CO})_4(^{13}\text{CO})(\text{CS})$ are assigned in a similar manner, except that the $a_1^{ax} \nu(\text{CO})$ mode (ν_2) has shifted from 2017 to 1979 cm^{-1} owing to the expected isotope effect.

Assignment of the Raman-active $\nu(\text{CO})$ modes presents a more difficult problem. Although four bands are expected in the CO stretching region, only two distinct features are observed in the solid-state Raman spectra of $\text{Cr}(\text{CO})_5(\text{CS})$ and $\text{W}(\text{CO})_5(\text{CS})$. For both complexes, the most intense band

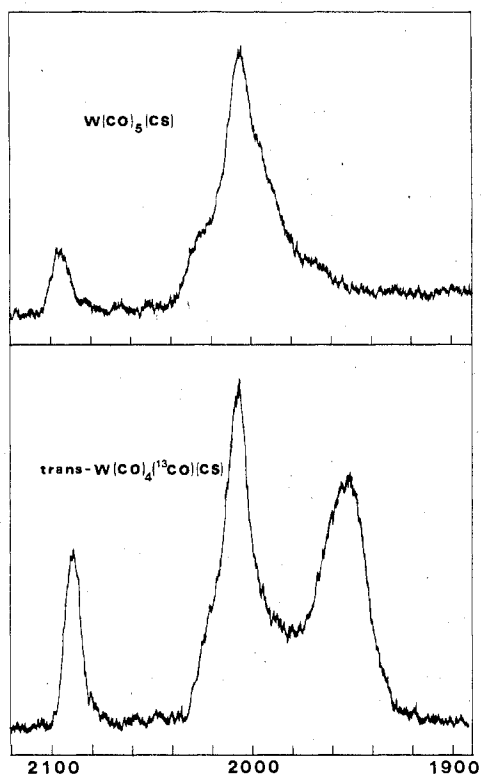


Figure 3. Solid-state Raman spectra of $W(CO)_5(CS)$ and $trans-W(CO)_4(^{13}CO)(CS)$ (90% ^{13}C enriched) in the CO stretching region. Experimental conditions: slit widths 2.5 cm^{-1} ; Kr^+ excitation, 647.1 nm (50 mW); -50°C .

Vib. type	$M(CO)_6 (O_h)$				$M(CO)_5(CS) (C_{4v})$				Vib. no.
	Vib. no.	$M = Cr$	$M = W$	Sym.	Sym.	$M = Cr$	$M = W$	$M = W$ ($trans-^{13}CO$)	
$\nu(CO)$	ν_1	2119	2126	A_{1g}	A_1	2107	2109	2103	ν_1
	ν_3	2027	2021	e_g	B_1	2018	2017	1977	ν_2
	ν_6	2000	1998	E_{1g}	B_2	1804	1805	1804	ν_3
$\nu(MC)$	ν_2	379	426	B_{1g}	B_1	419	419	419	ν_5
	ν_4	391	410	e_g	B_2	384	393	388	ν_6
	ν_8	440	374	E_{1u}	B_2	337	323	323	ν_7
	ν_{12}	440	374	E_{1u}	B_2	391	407	407	ν_{12}
$\delta[MCO(S)]$	ν_5	364	362	E_{1g}	B_1	419	375	374	ν_{20}
	ν_7	668	587	E_{1u}	B_2	666	588	587	ν_4
	ν_{10}	532	482	E_{2g}	B_2	367	350	350	ν_9
	ν_{12}	521	521	E_{2u}	B_2	510	520	520	ν_{11}
						531	487	487	ν_{14}
$\delta(MCS)$	ν_9	97	82	E_{1u}	B_1	665	580	577	ν_{17}
	ν_{11}	90	81	E_{2g}	B_2	527	508	499	ν_{18}
	ν_{13}	68	61	E_{2u}	B_2	492	468	468	ν_{19}
						345	336	335	ν_{21}

Figure 4. Correlation diagram between the $M(CO)_6$ (O_h symmetry) and $M(CO)_5(CS)$ (C_{4v} symmetry) molecules.

near 2000 cm^{-1} is broad and unsymmetric. By comparison with the ir spectra, it is reasonable to attribute these intense bands to ν_{16} . However, the e modes are not expected to be the most intense in the Raman spectra. The Raman spectrum of solid $trans-W(CO)_4(^{13}CO)(CS)$ exhibits three distinct peaks in the CO stretching region. The lowest energy band at 1954 cm^{-1} is assigned to the a_1^{ax} mode (^{13}CO , ν_2). This assignment necessitates a $1979 - 1954 = 25\text{ cm}^{-1}$ shift to lower energy for this mode in going from the gas-phase ir to the solid-state Raman. A similar large shift is not observed for the a_1^{eq} $\nu(CO)$ mode (ν_1). This suggests that the a_1^{ax} $\nu(CO)$ modes

in $Cr(CO)_5(CS)$ and $W(CO)_5(CS)$ undergo similar 25 cm^{-1} shifts in going from the gas-phase ir to the solid-state Raman, placing these modes at about 2007 and 1992 cm^{-1} , respectively, i.e., almost coincident with the e modes observed at $\sim 2000\text{ cm}^{-1}$. These accidental degeneracies would account for the unexpected intensities of the 2000 cm^{-1} bands because a_1 modes are usually the most intense in the Raman. The high-frequency shoulders on the 2000 cm^{-1} bands are assigned to the b_1 $\nu(CO)$ modes (ν_{10}): $Cr(CO)_5(CS)$, 2030 (2027 cm^{-1} calcd); $W(CO)_5(CS)$, 2025 (2025 cm^{-1} calcd). For $trans-W(CO)_4(^{13}CO)(CS)$, ν_{10} appears at 2022 cm^{-1} . Depolarization data for CH_2Cl_2 solutions of the $M(CO)_5(CS)$ complexes reveal the presence of two polarized bands near 2100 and 2000 cm^{-1} , thus confirming the location of the two expected a_1 $\nu(CO)$ modes.

CS Stretching Region ($1400\text{--}1200\text{ cm}^{-1}$). The only prominent feature in the gas-phase ir spectra of all three compounds throughout the $1900\text{--}700\text{ cm}^{-1}$ region appears at $\sim 1285\text{ cm}^{-1}$. These peaks are attributed to the a_1 $\nu(CS)$ modes (ν_3): $Cr(CO)_5(CS)$, 1280 ; $W(CO)_5(CS)$, 1286 ; $trans-W(CO)_4(^{13}CO)(CS)$, 1284 cm^{-1} . Although the energies of $\nu(CS)$ modes in transition metal thiocarbonyls range widely ($1403\text{--}1161\text{ cm}^{-1}$) depending upon the metal, its oxidation state, and the other ligands present, these modes are always extremely intense in the ir.¹⁹

In contrast to the ir, the $\nu(CS)$ modes in the solid-state Raman spectra are extremely weak and broad: $Cr(CO)_5(CS)$, 1260 ; $W(CO)_5(CS)$, 1261 ; $trans-W(CO)_4(^{13}CO)(CS)$, 1264 cm^{-1} . In all three cases, the bands are unsymmetric due probably to factor group effects.²⁰ The CH_2Cl_2 solution Raman spectrum of $W(CO)_5(CS)$ exhibits a polarized band at 1269 cm^{-1} , i.e., just in between the gas-phase ir and solid-state Raman values. As expected, because the dipole moments of the CS and axial CO groups lie along the same fourfold axis, the phase dependence of the vibrations associated with these groups is quite similar.

The lack of strong Raman activity for the $\nu(CS)$ modes in numerous transition metal thiocarbonyls^{7,21} is surprising in view of the high polarizability expected for the CS bonds. Because of the known chemistry of these complexes,^{4,8} we initially felt that the lack of Raman activity resulted from a polar



bond in these complexes.²¹ However, on the basis of photoelectron spectra for $Cr(CO)_5(CS)$, $W(CO)_5(CS)$, and $\eta^5-C_5H_5Mn(CO)_2(CS)$, together with molecular orbital calculations for the chromium and manganese complexes, Lichtenberger and Fenske²² have now put forward a more quantitative explanation for the diminished $\nu(CS)$ Raman intensities in these complexes. Their study reveals that the empty π^* levels of the CS ligands are coupled to the filled π levels through the metal π levels. As a result of the CS stretch, the CS π^* orbitals are lowered in energy and increase their carbon character, thus increasing their interaction with the metal π orbitals. Stretching destabilizes the CS π orbitals and decreases their carbon character, thus leading to a reduced interaction with the metal π orbitals. The net result of these two competing effects is a reduction in the change of polarizability along the CS bonds, and since the intensity of a Raman band is directly proportional to the square of the polarizability change, the intensities of the $\nu(CS)$ modes will be weak, as is observed.

$700\text{--}300\text{ cm}^{-1}$ Region. From the correlation diagram in Figure 4, four types of vibration are expected for the $M(CO)_5(CS)$ molecules in this region: $\nu[M-C(O)]$ ($2a_1 + b_1 + e$), $\nu[M-C(S)]$ (a_1), $\delta(MCO)$ ($a_1 + a_2 + b_1 + b_2 + 3e$), and $\delta(MCS)$ (e). In view of the complexity of this region, the

Table II. Comparison of Observed and Calculated Frequencies (cm^{-1}) for $\text{M}(\text{CO})_5(\text{CS})$ and $\text{trans-W}(\text{CO})_4(^{13}\text{CO})(\text{CS})$

Vib no.	$\text{Cr}(\text{CO})_5(\text{CS})$			$\text{W}(\text{CO})_5(\text{CS})$			$\text{trans-W}(\text{CO})_4(^{13}\text{CO})(\text{CS})$		
	Input	Calcd ^a	Calcd ^b	Input	Calcd ^a	Calcd ^b	Input	Calcd ^a	Calcd ^b
ν_1	2097 ir	2107	2106	2102 ir	2109	2106	2102 ir	2103	2100
ν_2	2032 ir	2018	2029	2017 ir	2017	2018	1979 ir	1977	1978
ν_3	1280 ir	1804	1280	1286 ir	1805	1285	1284 ir	1804	1285
ν_4	668 ir	666	668	584 ir	588	577		587	577
ν_5	424 R	419	424	426 R	419	418	425 R	419	418
ν_6	380 R	384	386	380 R	393	381	371 R	388	376
ν_7	351 R	337	351	346 R	323	343	345 R	323	343
ν_8	93 R	92	93		76	74		76	74
ν_9	364 ir	367	361		360	341		360	341
ν_{10}		2027	2027		2025	2025		2025	2025
ν_{11}	512 R	510	507	518 R	520	508	513 R	520	508
ν_{12}	390 R	391	392	412 R	407	407		407	407
ν_{13}		69	69		64	63		64	63
ν_{14}	526 R	531	527	479 R	487	473		487	473
ν_{15}		93	92		77	75		77	75
ν_{16}	2007 ir	2001	2000	2002 ir	2003	2003	2006 ir	2003	2003
ν_{17}	649 ir	665	662	569 ir	580	572	574 R	577	568
ν_{18}	526 R	527	523	491 R	508	497	483 R	499	489
ν_{19}	489 R	492	489	461 R	468	462	463 R	468	461
ν_{20}	424 ir	419	419	374 R	375	373		374	373
ν_{21}	340 R	345	340	332 R	336	329	331 R	335	327
ν_{22}		94	94		77	74		77	74
ν_{23}		83	82		70	69		70	69
ν_{24}		59	59		53	53		53	53
Av error, %		3.9 (0.85) ^c	0.42		3.2 (1.5) ^c	0.76		4.3 (0.92) ^c	0.75

^a Using the $\text{M}(\text{CO})_6$ force fields, see text. ^b Using the refined force field, see text. ^c The first value of the average percent error between observed and calculated frequencies includes the error in the $\nu(\text{CS})$ mode (ν_3), while the second value shown in parentheses does not.

"calculated" frequencies must be relied upon heavily, although relative intensity considerations place additional limits on the possible assignments of the observed spectra. Since these modes will be extensively mixed, the final assignments must await the potential energy distributions from the complete calculations to be discussed later. The following points were helpful in assigning this region. (1) The a_1 modes should dominate the Raman spectra, while the e modes should be the most intense in the ir. (2) The bending modes should be more intense than the stretching modes in the ir, while the reverse should be true in the Raman.⁷ (3) The b_1 and b_2 modes should only appear in the Raman spectra.

There are three intense bands in the Raman spectrum of solid $\text{Cr}(\text{CO})_5(\text{CS})$ at 424, 381, and 351 cm^{-1} . The corresponding bands in the CH_2Cl_2 solution spectrum are strongly polarized indicating that these modes have a_1 symmetry. Similarly, the solid-state Raman spectrum of $\text{W}(\text{CO})_5(\text{CS})$ also exhibits three intense bands at 426, 380, and 346 cm^{-1} . In the case of $\text{trans-W}(\text{CO})_4(^{13}\text{CO})(\text{CS})$, the first and third bands are unshifted, while the second band drops to 371 cm^{-1} . The small shift in the middle band suggests that all three intermediate bands should be assigned to the $a_1 \nu[\text{M}-\text{C}(\text{O})]^{ax}$ mode (ν_6). The mass effect of sulfur suggests that the bands at $\sim 350 \text{ cm}^{-1}$ are due to the $a_1 \nu[\text{M}-\text{C}(\text{S})]$ mode (ν_7). The "calculated" frequencies reveal that several modes will be accidentally degenerate, e.g., in $\text{Cr}(\text{CO})_5(\text{CS})$, both ν_5 and ν_{20} are predicted at 419 cm^{-1} . Therefore, the intense Raman band for solid $\text{Cr}(\text{CO})_5(\text{CS})$ at 424 cm^{-1} is assigned to the $a_1 \nu[\text{Cr}-\text{C}(\text{O})]^{eq}$ mode (ν_5), while the strong ir band for the vapor at 424 cm^{-1} is assigned to the $e \nu[\text{Cr}-\text{C}(\text{O})]$ mode (ν_{20}). All other such coincidences are noted beneath Table I. The assignments of the remaining bands in the 700–300 cm^{-1} region follow from the three points mentioned above and the "calculated" frequencies.

Normal Coordinate Calculations. As one of the prime purposes of the present study was to compare the nature of the $\text{M}-\text{C}(\text{S})$ and $\text{M}-\text{C}(\text{O})$ bonding in the $\text{M}(\text{CO})_5(\text{CS})$ molecules, we refined the metal hexacarbonyl force fields to fit the frequencies observed for the thiocarbonyls. During the

Table III. Potential Energy Distributions^{a,b}

$\text{Cr}(\text{CO})_5(\text{CS})$		$\text{W}(\text{CO})_5(\text{CS})^c$	
a_1 Species		a_1 Species	
ν_1	$0.75S_1 + 0.21S_2 + 0.04S_6$	ν_1	$0.79S_1 + 0.16S_2 + 0.05S_5$
ν_2	$0.23S_1 + 0.80S_2 + 0.03S_5$	ν_2	$0.18S_1 + 0.85S_2 + 0.04S_6$
ν_3	$0.94S_3 + 0.19S_7$	ν_3	$0.95S_3 + 0.19S_6$
	$-0.13S_{3,7}$		$-0.14S_{3,6}$
ν_4	$0.35S_4 + 0.11S_5 + 0.10S_6$	ν_4	$0.42S_4 + 0.21S_8$
	$+0.21S_8 + 0.20S_{4,8}$		$+0.33S_{4,8}$
ν_5	$0.24S_4 + 0.51S_5 + 0.27S_7$	ν_5	$0.03S_1 + 0.01S_5 + 0.93S_6$
	$-0.14S_{5,7}$		
ν_6	$0.02S_1 + 0.94S_6 + 0.01S_7$	ν_6	$0.02S_3 + 0.01S_4 + 0.90S_5$
			$+0.02S_6$
ν_7	$0.07S_3 + 0.31S_5 + 0.23S_6$	ν_7	$0.06S_3 + 0.03S_4 + 0.06S_5$
	$+0.40S_7 + 0.14S_{5,7}$		$+0.84S_7$
ν_8	$0.62S_4 + 0.18S_5 + 0.18S_7$	ν_8	$1.15S_4 + 0.18S_5 + 0.16S_7$
	$+1.08S_8 - 0.60S_{4,8}$		$+1.47S_8 - 1.45S_{4,8}$
	$-0.16S_{5,8} - 0.14S_{7,8}$		$-0.16S_{5,8} - 0.13S_{7,8}$

^a The potential energy distributions for the other symmetry blocks are given in the supplementary material. The S_i used here denote the source of the potential energy contributions and the numerical values should not be taken as coefficients of the symmetry coordinates, S_i . Only values >0.01 are reported for the primary symmetry force constants and all values due to the interaction constants have been omitted for the sake of simplicity unless they are unusually large. Since only part of the potential energy distribution is shown, the sum of the contributions for any one mode does not equal unity, and for the CMC deformation modes the sum is much greater than unity. ^b Refer to Figure 1 for the definition of the symmetry coordinates. ^c Only changes can occur in the a_1 block for $\text{trans-W}(\text{CO})_4(^{13}\text{CO})(\text{CS})$. The only significant changes found are as follows: ν_1 , $0.89S_1 + 0.07S_2 + 0.05S_6$; ν_2 , $0.09S_1 + 0.94S_2 + 0.04S_5$.

refinements, all the coordinate interaction constants were held fixed at the appropriate $\text{M}(\text{CO})_6$ values, while the valence force constants were allowed to refine. Constraining the interaction constants requires that the CO, CS interaction constants are equivalent to the corresponding CO, CO values. This may be an unreasonable assumption, but in any case the CO, CS interactions are not well defined; even if they are set equal to zero, no change occurs in the overall fitting errors

Table IV. Observed Vapor Phase and Energy-Factored Calculated Ir Spectra in the $\nu(\text{CO})$ and $\nu(\text{CS})$ Regions of $\text{M}(\text{CO})_5(\text{CS})$ and $\text{trans-W}(\text{CO})_4(^{13}\text{CO})(\text{CS})$

Molecule and symmetry	Vib assign.	$\nu(\text{CO})$ and $\nu(\text{CS}), \text{cm}^{-1}$			
		$\text{Cr}(\text{CO})_5(\text{CS})$		$\text{W}(\text{CO})_5(\text{CS})$	
		Obsd	Calcd ^a	Obsd	Calcd ^b
All ¹² CO <i>C_{4v}</i>	<i>a₁^{eq}</i>	2097	2097	2102	2103
	<i>a₁^{ax}</i>	2032	2033	2017	2019
	<i>b₁</i>	Inact.	2009	Inact.	2030
	<i>e</i>	2007	2008	2006	2006
	<i>a₁(CS)</i>	1280	1280	1286	1287
Mono ¹³ CO (<i>trans</i>) ^c <i>C_{4v}</i>	<i>a₁^{eq}</i>	<i>d</i>	2097	2102	2100
	<i>a₁^{ax}</i>	1991	1988	1979	1977
	<i>b₁</i>	Inact.	2009	Inact.	2030
	<i>e</i>	<i>d</i>	2008	2006	2006
	<i>a₁(CS)</i>	<i>d</i>	1280	1284	1287

^a Associated force constants: $f_{\text{CO}}^{\text{eq}} = 16.65, f_{\text{CO}}^{\text{ax}} = 16.70, f_{\text{CS}} = 8.43, f_{\text{CO,CO}}^{\text{cis,eq}} = 0.36, f_{\text{CO,CO}}^{\text{cis,ax}} = 0.04, f_{\text{CO,CO}}^{\text{trans}} = 0.38 \text{ mdyn } \text{Å}^{-1}$. Also used as input was the *a₁* mode of *cis*- $\text{Cr}(\text{CO})_4(^{13}\text{CO})(\text{CS})$: obsd, 1971; calcd, 1971 cm^{-1} . Also observed at 1245 cm^{-1} was the *a₁*(CS) mode of $\text{Cr}(\text{CO})_5(^{13}\text{CS})$: calcd, 1245 cm^{-1} . ^b Associated force constants: $f_{\text{CO}}^{\text{eq}} = 16.71, f_{\text{CO}}^{\text{ax}} = 16.60, f_{\text{CS}} = 8.50, f_{\text{CO,CO}}^{\text{cis,eq}} = 0.27, f_{\text{CO,CO}}^{\text{cis,ax}} = 0.21, f_{\text{CO,CO}}^{\text{trans}} = 0.47 \text{ mdyn } \text{Å}^{-1}$. ^c The data for the *trans*- $\text{W}(\text{CO})_4(^{13}\text{CO})(\text{CS})$ species are for the 90% ¹³C-enriched species. The 1979- cm^{-1} band was also observed in the natural abundance spectrum. ^d Buried beneath a much stronger mode of the all-¹²CO species.

and the largest frequency change is $\sim 1 \text{ cm}^{-1}$ in the *a₁* $\nu(\text{CO})^{\text{eq}}$ mode (ν_1). Additional frequency data from isotopically substituted species such as $\text{M}(^{13}\text{CO})_5(\text{CS})$ are obviously needed in order to define the CO,CS interaction constants.

The observed frequencies and those calculated using the $\text{M}(\text{CO})_6$ force fields and the refined force fields are compared in Table II. The average percent errors in the frequency fits are excellent when considerations of the problems involved with solid-state data and anharmonicity are taken into account. The average percent errors using the $\text{M}(\text{CO})_6$ force fields without refinement are quite good when the errors in the CS stretching modes are removed; however, even then most of the differences

between the observed and calculated values are considerably greater than the experimental errors. This indicates that some changes are necessary in the force fields and subsequent refinement of the valence force constants leads to significantly better frequency fits. Although these fits could undoubtedly be improved further by allowing some of the interaction constants to refine, there are too many interactions and the choice as to which should be allowed to refine is extremely arbitrary. We did attempt to refine the CO,CS and $\text{M}-\text{C}(\text{O}), \text{M}-\text{C}(\text{S})$ interaction constants, but convergence could not be obtained.

The above results indicate that the $\text{M}(\text{CO})_6$ interaction constants can be transferred successfully to the $\text{M}(\text{CO})_5(\text{CS})$ molecules, as predicted by Jones et al.¹⁰ However, only a few of the valence force constants may be used. Certainly, the use of the $\text{M}(\text{CO})_6$ force fields to aid the assignment of the spectra of less symmetrical octahedral metal carbonyl complexes is a great advantage and this is a procedure which could be utilized extensively.

The potential energy distributions in terms of the symmetry coordinates for the $\text{M}(\text{CO})_5(\text{CS})$ species are shown in Table III. Only values in excess of 0.01 are reported. While most of the stretching vibrations can be associated with distinct, although mixed, internal stretching coordinates, the eigenvalues associated primarily with deformation modes are a mixture of both $\delta(\text{MCO})$ and $\delta(\text{CMC})$ symmetry coordinates. The CO and CS stretching modes are not mixed, but the CS stretching modes are appreciably mixed with $\nu[\text{M}-\text{C}(\text{S})]$. The slight mixing of the $\nu(\text{CO})$ modes with the $\nu[\text{M}-\text{C}(\text{O})]$ modes parallels the results for the $\text{M}(\text{CO})_6$ calculations.¹⁰ Little mixing occurs between the three *a₁* $\nu(\text{M}-\text{C})$ modes of $\text{W}(\text{CO})_5(\text{CS})$ and the proposed assignments are confirmed. For $\text{Cr}(\text{CO})_5(\text{CS})$, however, the $\nu[\text{Cr}-\text{C}(\text{O})]^{\text{ax}}$ mode is extensively mixed with $\nu[\text{Cr}-\text{C}(\text{S})]$ and the ordering of the $\nu[\text{Cr}-\text{C}(\text{O})]^{\text{ax}}$ and $\nu[\text{Cr}-\text{C}(\text{O})]^{\text{eq}}$ modes is reversed.

For comparison with the results of the complete calculations and as an aid in the assignment of several weak bands observed in the ir spectra due to isotopic species present in natural abundance, energy-factored force field calculations were also carried out. The results are shown in Table IV, together with

Table V. Comparison of Force Constants for $\text{M}(\text{CO})_6$ and $\text{M}(\text{CO})_5(\text{CS})^{\text{a,b}}$

$\text{Cr}(\text{CO})_6$		$\text{Cr}(\text{CO})_5(\text{CS})$		$\text{W}(\text{CO})_6$		$\text{W}(\text{CO})_5(\text{CS})$	
f_{CO}	16.73 (3)	$f_{\text{CO}}^{\text{eq}}$	16.71 (6)	f_{CO}	16.80 (2)	$f_{\text{CO}}^{\text{eq}}$	16.78 (2)
		$f_{\text{CO}}^{\text{ax}}$	17.01 (16)			$f_{\text{CO}}^{\text{ax}}$	16.88 (3)
		f_{CS}	8.01 (40)			f_{CS}	8.17 (5)
f_{CrC}	2.08 (8)	$f_{\text{CrC}}^{\text{eq}}$	2.10 (7)	f_{WC}	2.36 (4)	$f_{\text{WC}}^{\text{eq}}$	2.32 (2)
		$f_{\text{CrC}}^{\text{ax}}$	2.01 (38)			$f_{\text{WC}}^{\text{ax}}$	2.12 (6)
		$f_{\text{CrC}}^{\text{s}}$	2.62 (66)			f_{WC}^{s}	2.77 (9)
f_{α}	0.75 (1)	f_{α}	0.75	f_{α}	0.77 (1)	f_{α}	0.77
$f_{\alpha\alpha'}$	0.08 (1)	$f_{\alpha\alpha'}$	0.08	$f_{\alpha\alpha'}$	0.14 (1)	$f_{\alpha\alpha'}$	0.14
$f_{\alpha\alpha''}$	0.20 (1)	$f_{\alpha\alpha''}$	0.20	$f_{\alpha\alpha''}$	0.14 (2)	$f_{\alpha\alpha''}$	0.14
f_{β}	0.48 (7)	$f_{\beta}^{\text{ax}} = f_{\beta}^{\text{eq}}$	0.47 (2)	f_{β}	0.48 (5)	$f_{\beta}^{\text{ax}} = f_{\beta}^{\text{eq}}$	0.44 (1)
		f_{β}^{s}	0.47 (7)			f_{β}^{s}	0.53 (4)
$f_{\text{CO,CO}}^{\text{cis}}$	0.21 (1)	$f_{\text{CO,CO}}^{\text{cis,eq}} = f_{\text{CO,CO}}^{\text{cis,ax}}$	0.21	$f_{\text{CO,CO}}^{\text{cis}}$	0.16 (1)	$f_{\text{CO,CO}}^{\text{cis,eq}} = f_{\text{CO,CO}}^{\text{cis,ax}}$	0.16
$f_{\text{CO,CO}}^{\text{trans}}$	0.21 (3)	$= f_{\text{CO,CS}}^{\text{cis,eq}} = f_{\text{CO,CO}}^{\text{trans}}$ $= f_{\text{CO,CS}}^{\text{trans}}$		$f_{\text{CO,CO}}^{\text{trans}}$	0.12 (2)	$= f_{\text{CO,CS}}^{\text{cis,eq}} = f_{\text{CO,CO}}^{\text{trans}}$ $= f_{\text{CO,CS}}^{\text{trans}}$	0.12

^a Units: stretching and stretch-stretch interactions, $\text{mdyn } \text{Å}^{-1}$; bending and bend-bend interactions, $\text{mdyn } \text{Å rad}^{-2}$; stretch-bend interactions, mdyn rad^{-1} . ^b The values of the interaction constants for the $\text{M}(\text{CO})_5(\text{CS})$ species were transferred from the corresponding $\text{M}(\text{CO})_6$ species (gas-phase values), as given in ref 10 except for the CO and CMC interaction constants which were obtained by refinement of the $\text{M}(\text{CO})_6$ force fields to fit the anharmonic frequencies. The CMC bending force constants and the stretch-CMC interaction constants are not uniquely defined because of the redundancy condition. Jones et al.¹⁰ report linear combinations of these force constants. Since valence force constants were required, we refined $f_{\alpha}, f_{\alpha\alpha'},$ and $f_{\alpha\alpha''}$ to obtain "best fits" for the $\text{M}(\text{CO})_6$ data; the results were used in the $\text{M}(\text{CO})_5(\text{CS})$ calculations without further refinement. The assumptions necessary for the stretch-bend interaction constants are included below. Values of the interaction constants transferred from the metal hexacarbonyls are listed below. The parentheses indicate assumptions about the relative magnitude of the force constants within the linear combination were required to obtain the reported numerical value. The values for the chromium complex are given first: $f_{\text{MC,MC}}^{\text{cis}} = -0.019, -0.049; f_{\text{MC,MC}}^{\text{trans}} = 0.44, 0.56; f_{\text{MC,CO}} = 0.68, 0.79; f_{\text{MC,C'O}}^{\text{cis}} = -0.05, -0.08; f_{\text{MC,C'O}}^{\text{trans}} = -0.10, -0.12; f_{\beta\beta} = 0.09, 0.08; f_{\beta\beta''} = 0.00, 0.01; f_{\beta\beta'''} = -0.01, -0.04; (f_{\alpha\alpha''}) = 0.00, 0.00; (f_{\alpha\alpha'''}) = 0.18, 0.27; f_{\alpha\beta} = -0.10, -0.12; f_{\alpha\beta''} = -0.02, -0.05; f_{\alpha\beta'''} = -0.02, -0.04; f_{\text{CO},\beta} = 0.00, 0.00; f_{\text{MC},\beta} = -0.04, -0.04; (f_{\text{CO},\alpha}) = 0.00, 0.00; (f_{\text{CO},\alpha'}) = 0.00, 0.00; (f_{\text{MC},\alpha}) = -0.15, -0.15; (f_{\text{MC},\alpha'}) = 0.00, 0.00.$

the associated energy-factored force constants.²³ In these calculations, all the CO,CS interaction constants were assumed equal to zero which effectively factors the CO and CS stretching vibrations as well. This factoring is somewhat supported by the inability to refine any CO,CS interaction constants in either the complete or the energy-factored calculations, as well as the negligibly small effect observed when the CO,CS interactions were varied from zero to the CO,CO values, as discussed earlier. The agreement between the observed and calculated values for the *trans*-M(CO)₄(¹³CO)(CS) species is within ± 3 cm⁻¹, thus verifying the proposed assignments. In addition, the assignment of a band at 1245 cm⁻¹ to ν (CS) of Cr(CO)₅(¹³CS) seems reasonable.

The optimum force constants from the complete calculations for the M(CO)₅(CS) complexes are compared with those for the isoelectronic M(CO)₆ molecules in Table V. The dispersions in the force constants for W(CO)₅(CS) are significantly smaller than those for the chromium complex as a result of the additional vibrational data from *trans*-W(CO)₄(¹³CO)(CS). Substitution of CS for CO produces no effect on the equatorial CO and M-C force constants ($f_{CO^{eq}}$ and $f_{MC^{eq}}$) in going from M(CO)₆ to M(CO)₅(CS). However, there are appreciable changes in the axial CO and M-C force constants ($f_{CO^{ax}}$ and $f_{MC^{ax}}$), the former increase while the latter decrease. Furthermore, the M-C(S) force constants (f_{MC^s}) are much larger than any of the other M-C force constants. These observations are in complete agreement with the chemical evidence whereby increased labilization of the CO group *trans* to CS is observed.^{8,9,11} The larger M-C(S) force constants indicate increased stability of the M-C(S) bonds relative to the M-C(O) bonds with respect to substitution. This is also in agreement with the chemistry of metal thiocarbonyls in general; e.g., there is no evidence for CS substitution in M(CO)₅(CS)^{8,9,11} or η^5 -C₅H₅M'(CO)₂(CS) (M' = Mn, Re), whereas the CO groups are readily replaced by donor ligands.⁴ In addition, in the mass spectra of numerous η^5 -C₅H₅M'(CO)(CS)L derivatives, there is little or no intensity observed for the (P-CS)⁺ ions.²⁴ These results are all supportive of stronger metal-CS than metal-CO bonding in transition metal carbonyl-thiocarbonyls.

A comparison of the CS force constants, f_{CS} , determined in the energy factored calculation and in the full calculation with that characteristic of free CS (8.49 mdyin/Å)²⁵ is informative. The frequency of bonded CS is close to that of free CS (1272 cm⁻¹) and so little change in bond order is indicated if energy factoring is employed. However, when mechanical coupling with the other vibrational modes is allowed, as in the full calculation, a significant decrease is observed. In general, for an M-C-X linkage, as the mass of X and the force constant f_{CX} approach the mass of M and the force constant f_{MC} , respectively, the coupling of the vibrations will increase and the bond orders will not be reflected accurately by the observed frequencies. The observed frequency of the ligand bound to the metal, ν (CX), may increase relative to the free ligand while the associated force constant, f_{CX} , decreases.²⁶

It should be emphasized that the energy-factored force constants (Table V) do not reflect any significant differences between the axial and equatorial CO force constants ($f_{CO^{ax}}$ and $f_{CO^{eq}}$). In fact, the magnitudes of the force constants are reversed in going from Cr(CO)₅(CS) to W(CO)₅(CS). This also illustrates the dangers inherent in using approximate force constants to discuss bonding.

Since the equatorial CO and M-C force constants ($f_{CO^{eq}}$ and $f_{MC^{eq}}$) are unchanged in going from M(CO)₆ to M(CO)₅(CS), it seems reasonable to postulate that the extent of CO σ bonding is the same in both cases. It follows, therefore, that the labilization of the axial CO group in the M(CO)₅(CS) complexes must result principally from a

decrease in the $d\pi(M-C) \rightarrow \pi^*(CO)$ bonding for the axial CO group owing to the stronger π -acceptor capacity of the *trans* CS ligand. This conclusion is in agreement with the photoelectron studies and molecular orbital calculations on Cr(CO)₅(CS) and η^5 -C₅H₅Mn(CO)₂(CS) in which it was concluded that CS is both a better σ -donor and π -acceptor ligand than CO.²² However, on the basis of mass spectral data for (η^5 -C₅H₄R)Mn(CO)₂(CS) (R = H, Me), Efraty et al.⁵ have claimed that CS is a poorer π -acceptor ligand than CO. In view of the evidence to the contrary, these mass spectral results must be considered misleading, particularly since the conclusion was based on appearance potentials of the various fragment ions without a detailed knowledge of their structure.

Acknowledgment. This research was generously supported by the National Research Council of Canada and the Quebec Department of Education. We thank Professor R. J. Angelici and Mr. B. D. Dombek for giving us the samples of the thiocarbonyl complexes. One of us (A.G.-R.) thanks the Bank of Mexico for the award of a graduate scholarship.

Registry No. Cr(CO)₅(CS), 50358-90-2; W(CO)₅(CS), 50358-92-4; *trans*-W(CO)₄(¹³CO)(CS), 60172-96-5; Cr(CO)₆, 13007-92-6; W(CO)₆, 14040-11-0.

Supplementary Material Available: Complete version of Table III, listing the potential energy distributions for all the symmetry blocks of the M(CO)₅(CS) species (3 pages). Ordering information is given on any current masthead page.

References and Notes

- (1) Presented in part at the 4th International Meeting on Raman Spectroscopy, Bowdoin College, Maine, August 1974.
- (2) To whom correspondence should be addressed.
- (3) M. C. Baird and G. Wilkinson, *Chem. Commun.*, 267 (1966).
- (4) I. S. Butler and A. E. Fenster, *J. Organomet. Chem.*, **66**, 161 (1974).
- (5) For example, see A. Efraty, M. H. A. Huang, and C. A. Weston, *Inorg. Chem.*, **14**, 2799 (1975).
- (6) P. Caillet and G. Jaouen, *J. Organomet. Chem.*, **91**, C53 (1975).
- (7) G. G. Barna, I. S. Butler, and K. R. Plowman, *Can. J. Chem.*, **54**, 11 (1976).
- (8) B. D. Dombek and R. J. Angelici, *J. Am. Chem. Soc.*, **95**, 7516 (1973).
- (9) B. D. Dombek and R. J. Angelici, *Inorg. Chem.*, **15**, 1089 (1976).
- (10) L. H. Jones, R. S. McDowell, and M. Goldblatt, *Inorg. Chem.*, **8**, 2349 (1969).
- (11) B. D. Dombek and R. J. Angelici, *J. Am. Chem. Soc.*, **98**, 4110 (1976).
- (12) J. Overend and J. R. Scherer, *J. Chem. Phys.*, **32**, 1289 (1960); C. D. Needham, Ph.D. Thesis, University of Minnesota, Minneapolis, Minn., 1965.
- (13) R. J. Angelici and R. A. Jacobson, personal communication.
- (14) J. L. de Boer, D. Rogers, A. C. Skapski, and R. J. H. Troughton, *Chem. Commun.*, 756 (1966).
- (15) J. S. Field and P. J. Wheatley, *J. Chem. Soc., Dalton Trans.*, 2269 (1972).
- (16) I. S. Butler and C. F. Shaw III, *J. Mol. Struct.*, **31**, 359 (1976).
- (17) D. M. Adams, "Metal-Ligand and Related Vibrations", Arnold, London, 1967.
- (18) P. S. Braterman, "Metal Carbonyl Spectra", Academic Press, London, 1975.
- (19) I. S. Butler and D. A. Johansson, *Inorg. Chem.*, **14**, 701 (1975).
- (20) The M(CO)₆ complexes and Cr(CO)₅(CS) all crystallize in the *Pna*2₁ (*Z* = 4) space group (*C*_{2v}⁹). Since the metal hexacarbonyls are isomorphous, it is reasonable to expect W(CO)₅(CS) to be isomorphous with Cr(CO)₅(CS). From the correlation between *C*_{4v} molecular symmetry, *C*₁ site symmetry, and *C*_{2v} factor group symmetry, non-degenerate modes of the free M(CO)₅(CS) species could theoretically be split into four components (*a*₁ + *a*₂ + *b*₁ + *b*₂) in the crystal. All four of these components would be active in the Raman, while all but *a*₂ would be ir active. Therefore, we attribute the broadening and the asymmetry of the ν (CS) modes in the Raman to correlation effects. The splitting of the *a*₁^{ax} ν (CO) mode (ν_1) of Cr(CO)₅(CS) into two partially resolved components ($\Delta\nu \sim 3$ cm⁻¹) in the Raman spectrum of the solid at ca. -30 °C using 0.75 cm⁻¹ slits is similarly assigned.
- (21) C. F. Shaw III, I. S. Butler, and A. Garcia-Rodriguez, Abstracts, 168th National Meeting of the American Chemical Society, Atlantic City, N.J., 1974, No. INOR 14.
- (22) D. L. Lichtenberger and R. F. Fenske, submitted for publication.
- (23) F. A. Cotton and C. S. Kraihanzel, *J. Am. Chem. Soc.*, **84**, 4432 (1962).
- (24) I. S. Butler, N. J. Coville, D. Cozak, A. Garcia-Rodriguez, and T. Sawai, unpublished results.
- (25) L. H. Jones, "Inorganic Vibrational Spectroscopy", Marcel Dekker, New York, N.Y., 1971, p 185.
- (26) The stretching frequencies due primarily to the M-C(S) and C-S modes are also extremely sensitive to the interaction constants $f_{MC,CS}$, which were set equal to the interaction constants $f_{MC,CO}$ of the metal hex-

acarbonyls. While transference of $f_{\text{M-CO}}$ to the M-CO linkages in $\text{M}(\text{CO})_5(\text{CS})$ is certainly reasonable, this may be a poor approximation for the M-CS linkages. Consequently the f_{CS} and f_{MC} values contain

some uncertainty which cannot be removed given the present frequency data: ^{13}C substitution at the thiocarbonyl carbons is necessary to refine all the force constants in the M-CS linkages.

Contribution from the Department of Chemistry,
Florida State University, Tallahassee, Florida 32306

Lattice Effects on the Electron Resonance of Halopentaamminechromium(III) Complexes. Temperature Dependence

B. B. GARRETT* and M. T. HOLBROOK

Received March 1, 1976

AIC601535

The spin-Hamiltonian parameters of $[\text{Cr}(\text{NH}_3)_5\text{X}]$ in $[\text{Co}(\text{NH}_3)_5\text{X}]\text{Y}_2$ hosts ($\text{X} = \text{Cl}, \text{Br}; \text{Y}^- = \text{Cl}^-, \text{Br}^-, \text{I}^-, \text{NO}_3^-$) have been measured in the temperature range from 75 K to the decomposition temperature (430–550 K) and at 4 K. The nitrates show large changes near 130 K, while the halides have smooth variations over the entire temperature range. The implications of these data about the nature of lattice perturbations are discussed. Determination of the sign of the zero-field splitting from powder spectra is described.

Introduction

The effects of nearest-neighbor counterions on the electron resonance spectra of halopentaamminechromium complexes were examined in a previous study.¹ It was shown that at least two separate mechanisms were necessary to account for the variations in the zero-field splitting tensors of $[\text{Cr}(\text{NH}_3)_5\text{X}]\text{Y}_2$ ($\text{X} = \text{Cl}, \text{Br}; \text{Y}^- = \text{Cl}^-, \text{Br}^-, \text{I}^-, \text{NO}_3^-$) which were substituted into the isomorphous series of analogous cobalt hosts. The primary effect, a decrease of the axial parameter D with increased counterion size, was attributed to a variation of the orientation of repulsive forces between the counterions and the bound halide, which protrudes through the face of the roughly eightfold cubic arrangement of counterions. This mechanism can be visualized by noting the relative positions of the halides in the a - c projection of the orthorhombic unit cell of $[\text{Co}(\text{NH}_3)_5\text{Cl}]\text{Cl}_2$ shown in Figure 1. A larger counterion would be less effective in pushing the bound halide away from the metal, thereby leaving a more nearly cubic field at the metal site; thus the axial parameter, D , is smaller for larger counterions. A logical consequence of this mechanism would be a similar decrease in D with an increase in temperature because the larger thermal motions of the counterions will give a smaller average repulsion of the bound halide. This contrasts with an earlier observation that there was no difference in the EPR spectra at 77 and 300 K for $[\text{Cr}(\text{NH}_3)_5\text{Cl}]\text{Cl}_2$ in the analogous cobalt host.² But that observation was accidental as we shall see from the full temperature dependence of the spectra.

The second mechanism, which was associated with variations of the rhombic zero-field splitting parameter E , was not so well characterized in our counterion dependence study.¹ It was observed that E is larger with chloride and iodide counterions than with bromide and nitrate counterions, but no explanation was found. The $[\text{Co}(\text{NH}_3)_5\text{Cl}]\text{Cl}_2$ host is measurably nonaxial at the cobalt site as seen from the positions³ and thermal ellipsoids of the nitrogen atoms in the crystal lattice.¹ The quadrupole asymmetry parameter $\eta = 0.25$ for ^{59}Co in this lattice⁴ has a larger nonaxiality than the chromium guest which has an analogous EPR asymmetry parameter $3E/D = 0.15$. Since no intramolecular origin for E exists, the rhombic parameter E is entirely of lattice origin and shows a large variation with the nature of the counterion. As with the axial parameter, the temperature dependence may be useful in elucidating the origin of the rhombic parameter in these systems.

There have been a number of studies⁴⁻¹¹ on lattice motions in aminocobalt complexes using nuclear resonance of protons, deuterons, and chlorine and cobalt nuclei, and these motions may have some bearing on the temperature variations of the electron resonances studied here. These studies have shown that threefold rotations of the amines usually persist even at liquid nitrogen temperature unless some specific hydrogen-bonding interaction restricts the process.⁵⁻⁹ Whole complex ion rotations can begin above 200 K provided that the motion does not interchange ammine ligands with halogen ligands. Such whole ion motions have been observed^{5,7,8} for $[\text{Co}(\text{NH}_3)_6]^{3+}$, $[\text{Co}(\text{NH}_3)_5\text{H}_2\text{O}]^{3+}$, and *trans*- $[\text{Co}(\text{NH}_3)_4\text{Cl}_2]^+$ but not for *cis*- $[\text{Co}(\text{NH}_3)_4\text{Cl}_2]$.^{10,11} Surprisingly, whole ion motions have not been observed for $[\text{Co}(\text{NH}_3)_5\text{X}]\text{Y}_2$; $[\text{Co}(\text{NH}_3)_5\text{Cl}]\text{Br}_2$ and $[\text{Co}(\text{NH}_3)_5\text{Br}]\text{Br}_2$ exhibit only the threefold ammine rotations over the range from 110 to 350 K.⁶ Thus, in the host lattices used in the present study and presumably for the guest chromium complexes as well, the ammine ligands are undergoing rotations about the bond axis which are sufficiently fast to average the proton dipole-dipole interaction. It is also notable that at ambient temperatures the bound chlorine quadrupole resonance was not observable in $[\text{Co}(\text{NH}_3)_5\text{Cl}]\text{Cl}_2$ even though the cobalt resonances were seen, while both types of resonance were seen under similar conditions in the $[\text{Co}(\text{NH}_3)_5\text{Cl}]\text{SO}_4\cdot\text{H}_2\text{SO}_4$.⁴ This indicates an unusual relaxation time which may be associated with contact repulsions.

Methods and Results

Starting materials $[\text{Cr}(\text{NH}_3)_5\text{Cl}]\text{Cl}_2$, $[\text{Cr}(\text{NH}_3)_5\text{Br}]\text{Br}_2$, and $[\text{Co}(\text{NH}_3)_5\text{Br}]\text{Br}_2$ were made via standard preparations involving the heating of the aquopentaammine or carbonatopentaammine complexes in the presence of HCl or HBr.¹²⁻¹⁴ $[\text{Co}(\text{NH}_3)_5\text{Cl}]\text{Cl}_2$ was obtained commercially and recrystallized several times from a minimum amount of water. Each compound was ground with cold concentrated H_2SO_4 until HCl or HBr ceased to evolve. The very soluble sulfate or bisulfate salt of the complex was dissolved in water and reprecipitated with excess H_2SO_4 . Mixed crystals were obtained by dissolving about 0.006 g of the chromium salt with about 0.3 g of the cobalt salt in 50 ml of water in an ice bath and saturating the solution with the sodium or potassium salt of the desired counterion. Dry air was then passed over the 0 °C solution for approximately 24 h. The crystals were filtered, washed with ethanol and ether, and allowed to air-dry before being ground into a very fine powder for placement in